

**OPEN ACCESS**

## Microstructure of creep-exposed single crystal nickel base superalloy CSMX4

To cite this article: P Strunz *et al* 2010 *J. Phys.: Conf. Ser.* **247** 012039

View the [article online](#) for updates and enhancements.

### You may also like

- [Control of Inconel 738LC superalloy microstructure with the aid of a precipitate dissolution semi-analytical modeling](#)  
Yann Danis, Corinne Arvieu, Eric Lacoste et al.
- [Effects of alloying element and temperature on the stacking fault energies of dilute Ni-base superalloys](#)  
S L Shang, C L Zacherl, H Z Fang et al.
- [Growth Mechanisms of Oxide Scales on Two-phase Co/Ni-base Model Alloys between 800 °C and 900 °C](#)  
Martin Weiser, Mathias C. Galetz, Richard J. Chater et al.



**ECS**  
The  
Electrochemical  
Society  
Advancing solid state &  
electrochemical science & technology

**DISCOVER**  
how sustainability  
intersects with  
electrochemistry & solid  
state science research

# Microstructure of creep-exposed single crystal nickel base superalloy CSMX4

P Strunz<sup>1,2</sup>, J Zrník<sup>3,4</sup>, A Epishin<sup>5</sup>, T Link<sup>6</sup>, S Balog<sup>7</sup>

<sup>1</sup> Nuclear Physics Institute, CZ-25068 Řež near Prague, Czech Republic

<sup>2</sup> Research Centre Řež, CZ-25068 Řež near Prague, Czech Republic

<sup>3</sup> Technical University of Košice, Department of Materials Science, Slovakia

<sup>4</sup> COMTES FHT Inc., CZ-33441 Dobřany, Czech Republic

<sup>5</sup> Federal Institute for Materials Research and Testing, Unter den Eichen 87, 12205 Berlin, Germany

<sup>6</sup> Technical University Berlin, 10623 Berlin, Germany

<sup>7</sup> Laboratory for Neutron Scattering, PSI & ETH Zürich, CH-5232 Villigen, Switzerland

E-mail: strunz@ujf.cas.cz

**Abstract.** Main changes which appear in microstructure of Ni base superalloys during creep exposure is the directional coarsening (rafting) of originally cubic  $\gamma'$  precipitates embedded in  $\gamma$  matrix. The progress in  $\gamma'$  degradation can be assessed with help of the analysis of geometrical parameters of the  $\gamma'$  microstructure. Determination of the morphological changes of  $\gamma'$  in creep-exposed single-crystal Ni-base superalloy CMSX4 using SANS was carried out. A new sample design (conic specimen) was tested in order to get continually changing stress levels in one sample and corresponding variety of microstructural change. Evolution of rafts with stress magnitude is clearly observable from the parameters obtained using SANS (the mean thickness of the  $\gamma$  channel in different crystallographic directions of the single-crystal, the evolution of the  $\gamma'$  precipitate size and distance, the evolution of the specific interface). The use of conic specimen and spatial scan facilitate determination of microstructure evolution in dependence on the exposure parameters.

## 1. Introduction

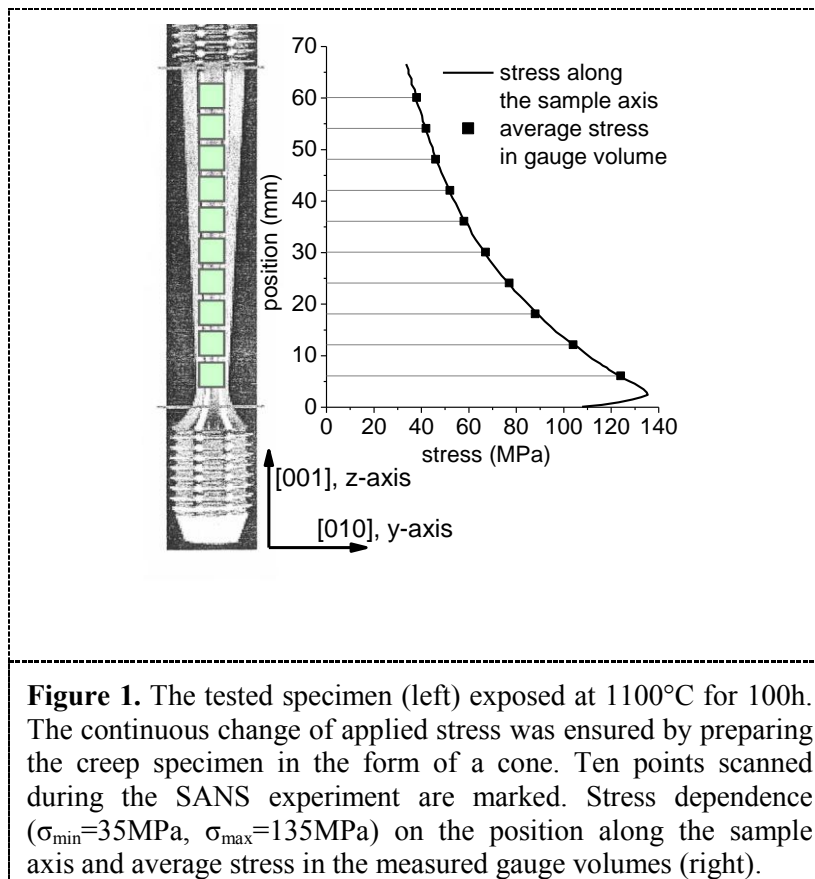
Turbine blades in gas turbines, fabricated of Ni base superalloys, operate under the creep and creep-fatigue conditions. One of the main changes which appear in microstructure during creep exposure is the directional coarsening (rafting) of originally cubic  $\gamma'$  precipitates embedded in  $\gamma$  matrix. For residual lifetime estimation, it is desirable to have a non-destructive method which could reliably evaluate the progress in  $\gamma'$  degradation in dependence on exposure time and relate these changes to the magnitude of stress the blade is experiencing. The available literature indicates that necessary information can be obtained from the analysis of geometrical parameters of the  $\gamma'$  microstructure and  $\gamma/\gamma'$  misfit [1, 2]. Using the bulk sensitive small-angle neutron scattering (SANS), morphological changes of  $\gamma'$  phase resulting from the operation condition can be detected. SANS method [3] has proved to contribute successfully to the morphology assessment of  $\gamma'$  in nickel base superalloys [4-8].

The aim of this investigation was to evaluate the morphological changes of  $\gamma'$  in creep-exposed single-crystal Ni-base superalloy CMSX4 and relate them to the various applied stress levels. The secondary aim of the experiment was to test a possibility to investigate the microstructural parameters using a new special sample design: a conic specimen. As a result of the diameter change along the longitudinal axis, a continuous change of applied stress magnitude acting during the creep test exists which causes different microstructural change at different positions along the specimen.

## 2. Experimental

Currently, the most widely used material for high pressure propulsion turbines is single-crystal Ni-base superalloy CMSX-4 (the representative of the 2nd generation of single-crystal nickel base superalloys) with increased content of Re which strengthens the  $\gamma'$  precipitates and retards their coarsening [9]. The alloy underwent the following heat treatment: solutioning at 1581K/18h/AC (gas-fan quenched) + 1413K/6h/AC + 1145K/24h/AC, which led to large volume fraction ( $\approx 70\%$ ) of cubic  $\gamma'$ -precipitates.

Then, the conic specimen (Fig. 1, left) of CMSX-4 was exposed to a maximum stress 135 MPa for 100h under uniaxial tensile creep load along [001] direction (the temperature during the creep was held constant at 1100°C). The conic shape of the specimen enabled to receive various stress levels along the specimen axis (Fig. 1, right). The resulting stress was calculated from the known load and sample geometry. Afterwards, a slice was cut from the specimen along the vertical axis (i.e. [001]) in order to produce a sample of an appropriate thickness ( $\approx 2.5$  mm) for the ex-situ SANS experiment. Thus, the spatial scan of the sample could depict microstructure for exposures between 35 and 135 MPa.



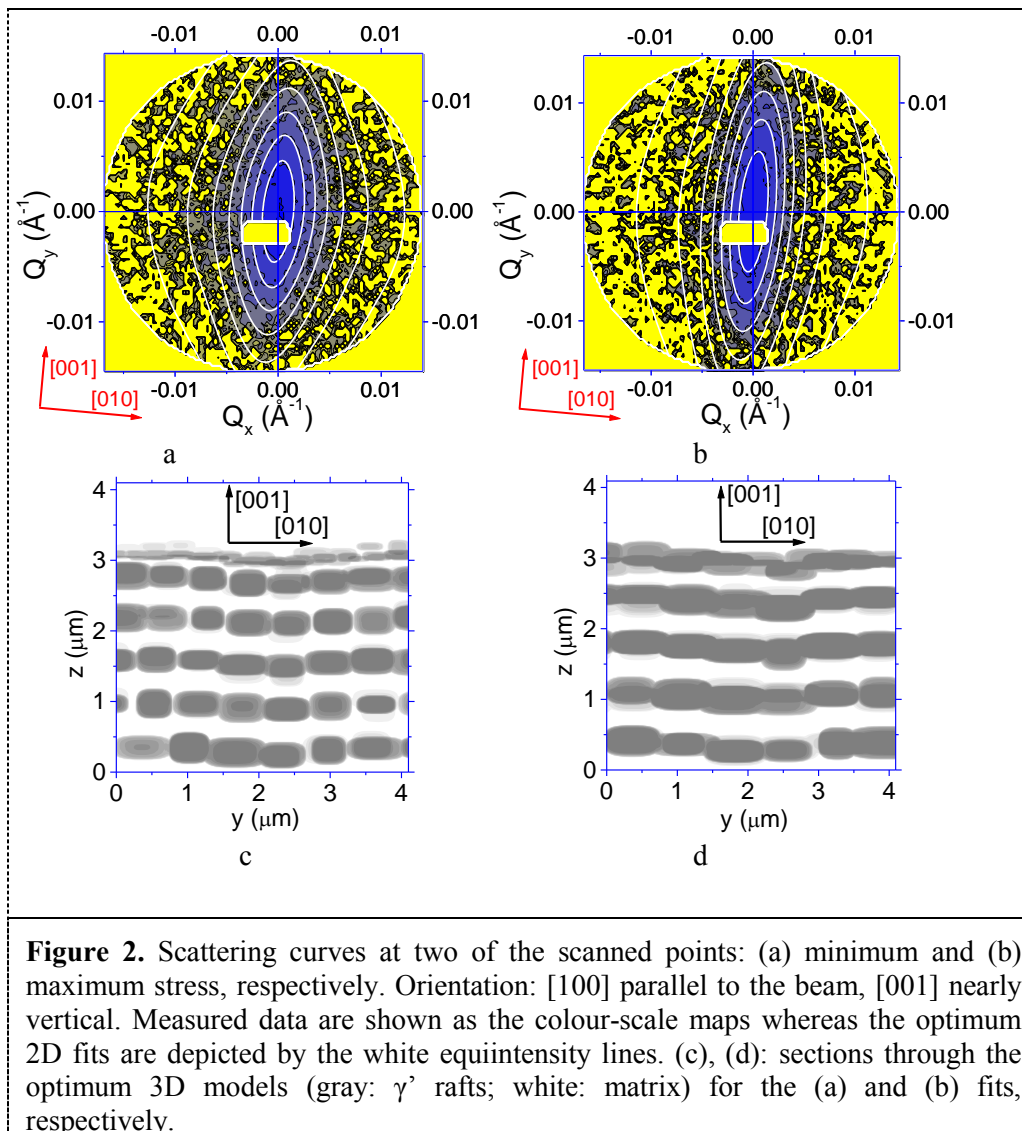
SANS measurement was carried out at the SANS II instrument of SINQ user lab of Paul Scherrer Institute, Villigen, Switzerland [10], which is equipped with a two-dimensional (2D) position sensitive detector. The samples were first oriented ( $\omega$ -scan, tilt) in such a way that the [100] crystallographic direction was parallel to the beam and the [001] crystallographic direction was vertical.

The spatial adjustment into the beam was done using linear table. The sample (Fig. 1) was scanned in vertical direction (i.e. along [001]) at room temperature. The used small slit (height 5.2 mm, width 4.9 mm) ensured that the morphology gradient within the gauge volume ( $\approx 50 \text{ mm}^3$ ) is not excessively large.

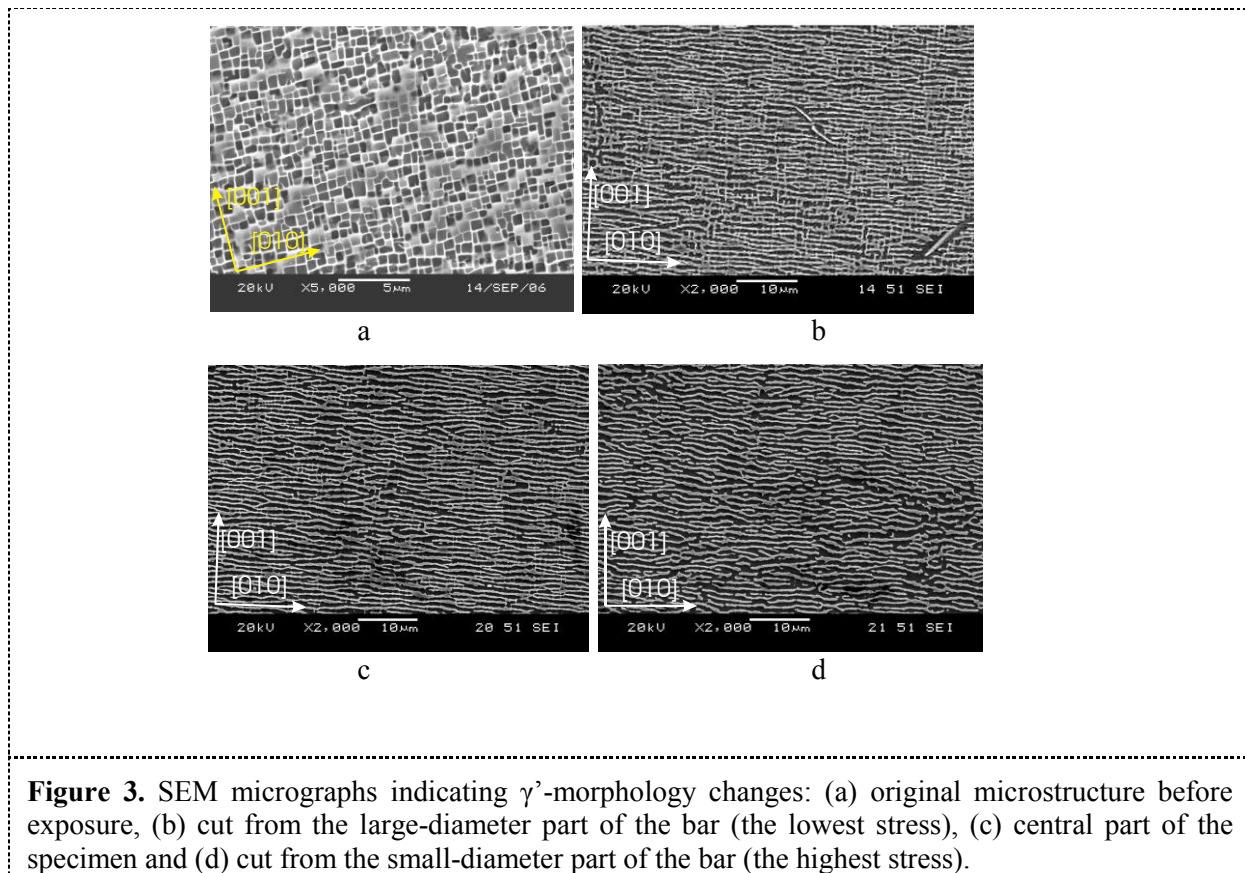
The scattering data were collected at several geometries (the sample-to-detector distance varied from 1 m to 6 m, and the neutron wavelength  $\lambda$  from 4.55 Å to 19.6 Å). The covered range of the scattering vector  $\mathbf{Q}$  was  $1.2 \times 10^{-3} \text{ \AA}^{-1}$  to  $0.3 \text{ \AA}^{-1}$  (i.e.  $1.2 \times 10^{-2} \text{ nm}^{-1} < Q < 3 \text{ nm}^{-1}$ ), where the magnitude  $Q = |\mathbf{Q}| = |\mathbf{k} - \mathbf{k}_0|$ ,  $\mathbf{k}_0$  and  $\mathbf{k}$  being the wave vectors of incident and scattered neutrons, respectively, and  $|\mathbf{k}| = |\mathbf{k}_0| = 2\pi/\lambda$  due to the elastic scattering. The measured raw data were corrected for background scattering, sample volume and normalized to the macroscopic differential cross section [3]. The data measured at large  $Q$ -magnitudes indicated the presence of a second population of  $\gamma'$  precipitates of cuboidal shape with size about 10 nm. These were formed in the  $\gamma$ -phase channels on cooling from the high temperature. The most interesting- from the point of view of rafting - is, however, the measurement performed at very low  $Q$ -magnitudes as it brings out information on the rafting process of the original large cubic precipitates.

### 3. Results

The two of the obtained 2D scattering curves (for  $\sigma = 38$  and 124 MPa) are displayed in Figs. 2a and 2b. They were taken at the opposite ends of the SANS sample (the most top and the most bottom scanned areas shown in Fig. 1). All the other scattering curves taken at the points in between these two extremes exhibit a continuous change of the  $\gamma'$  shape. Therefore, only two extreme cases are displayed. Nevertheless, all then scanned points were equally evaluated and provide thus dependencies of microstructural parameters on the stress level.



The remaining part of the specimen, not used for SANS sample, was investigated by SEM in order to analyze microstructural change of  $\gamma'$ . SEM micrographs (presented in Fig. 3) indicate still partially non-rafted microstructure in the part of the bar exposed to the lowest stress, while the highest stress causes already advanced rafting.



Qualitatively, the 2D scattering curves confirm the results of the electron microscopy performed on the specimen from the same bar.

#### 4. Microstructural parameters evaluation

SANS results were used to evaluate the change of microstructural parameters of the  $\gamma'$  phase along the conic specimen. Collected scattering data were processed with a numerical modelling technique [11] based on the simulation of a scattering profile generated from a three-dimensional (3D) microstructural model of a particle system. Thus, the modelled scattering curve also covers the interparticle-interference effect. Moreover, multiple scattering corrections [12] are included as well in this procedure. The calculated 2D profile is then matched with the experimental curve in order to find microstructural parameters.

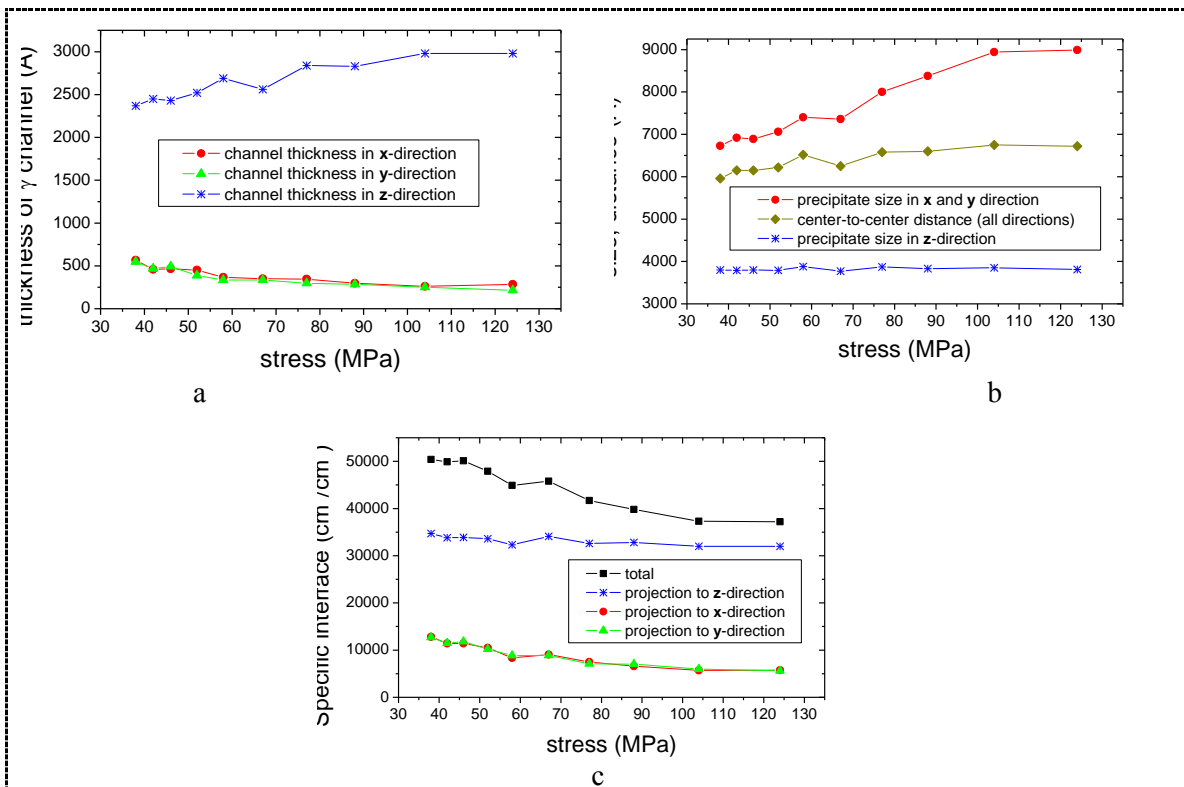
A model of (partially) agglomerated  $\gamma'$ -precipitates was employed for the modelling of rafting. Due to the large size of the precipitates in the order of  $\mu\text{m}$ , the measured data does not provide direct information on their size as well as on the distance between them. However, the information of the  $\gamma$  channel thickness between precipitates can be obtained as it is significantly smaller. Then, the relative change of size and distance of precipitates itself can be calculated from the model providing that the volume fraction is known. As the thermal history of the sample is identical at all the locations, an assumption was made that the volume fraction of large precipitates is the same for all the scanned points. The constant volume fraction 55% was used for the modelling. If correct, then the absolute distance and size of precipitates in the respective directions could be obtained. As we do not know the actual volume fraction, however, we can take the reported size and distance parameters evolution only as a relative measure of the real size and distance.

Fig. 2c and 2d display two models corresponding to the optimum fits to the SANS data for the two scanned points at opposite ends of the conic specimen.

The detailed evaluation of the data has brought a series of morphological parameters in dependence on the applied stress. In Fig. 4, the evolution of various parameters with the stress level is depicted. As can be seen from the evolution of the channel thickness (Fig. 4a), various extent of rafting of  $\gamma'$  precipitates embedded in the  $\gamma$  phase matrix was observed at variously exposed positions inside the sample. The tendency corresponds to the expected evolution: the larger stress, the more advanced rafting process. However, the used conditions for exposing the CMSX-4 single crystal do not allow to observe initial stages of rafting process, as can be seen from already large split of the thickness in x- and y- direction on one side and in z-direction on the other, even at the lowest applied stress level.

The relative change of the size and distance of precipitates can be observed in Fig. 4b. As the precipitate size in x- and y-directions is larger than the average distance between the precipitates in these directions (see overlapping precipitates in Fig. 2d), a clear occurrence of rafting can be deduced also from these parameters.

The last graph, Fig. 4c, displays the evolution of the specific interface between  $\gamma$  and  $\gamma'$  phase. The total specific interface as well as its projections to x, y and z-directions decrease with the stress level, as expected. The more pronounced is the decrease of the projection into x- and y-directions than into z-direction, as the former is caused by the disappearance of  $\gamma$  channels in [001] direction during the rafting process. Comparison between magnitudes in the respective directions confirms that the rafting advanced even for the lowest stress. The determined total specific interface between to be 37000 and 50000  $\text{cm}^2/\text{cm}^3$  can be used only as indication of the real absolute value as it depends on the input volume fraction as described above.



**Figure 4.** Resulting evolution of parameters. (a) the mean thickness of the  $\gamma'$  channel in the respective directions (x-direction is [100], y-direction is [010] and z-direction is [001]), (b) the relative evolution of the average precipitate size and distance, (c) the relative evolution of the specific interface - total and projection to the respective directions.

## 5. Conclusions

A different extent of  $\gamma'$ -precipitates rafting was observed for variously exposed positions inside the conic specimen. Evolution of rafts with stress level is clearly observable from the parameters obtained from SANS curves. The tendency corresponds to the expected evolution: the larger stress, the more advanced rafting process. Qualitatively, the 2D scattering curves confirmed the results of the electron microscopy performed on the specimen from the same bar.

The use of conic specimen and spatial scan largely facilitate determination of microstructure evolution in dependence on exposure parameters. The detailed evaluation of the SANS data brought a series of morphological parameters in dependence on the applied stress, particularly the mean thickness of the  $\gamma$  channel in the respective crystallographic directions ([100], [010] and [001]) of the single-crystal CMSX-4 specimen, the evolution of the  $\gamma'$  precipitate size and distance as well as the evolution of the specific interface.

The results confirmed that SANS method can be a proper non-destructive method for evaluation of structural changes caused by creep exposure in Ni base superalloys.

## Acknowledgments

This research project was supported by EC under the FP6 (Key Action: Strengthening the European Research Infrastructures), contract No. RII3-CT-2003-505925 (NMI3). P. Strunz gratefully acknowledges support by MSM2672244501 and IRP AV0Z10480505 projects.

## References

- [1] Mughrabi H, Biermann H, Ungar T 1992 *Superalloys 1992*, (Warrendale, PA: TMS) p 599
- [2] Link T, Epishin A, Brickner U, Portella P D 2000 *Acta Mater.* **8** 1981
- [3] Kostorz G 1979 *Neutron Scattering*, ed. G Kostorz (New York: Academic Press) p 227-289
- [4] Zrník J, Strunz P, Horňák P, Vrchovinský V, Wiedenmann A 2002 *Applied Physics A* **74** 1155
- [5] Zickler G A, Schnitzer R, Radis R, Hochfellner R, Schweins R, Stockinger M and Leitner H 2009 *Mat. Sci. Eng. A* **523** 295-303
- [6] Gilles R 2005 *Zeitschrift für Metallkunde* **96** 325-334
- [7] Ratel N, Deme B, Bastie P and Caron P 2008 *Scripta Materialia* **59** 1167-1170
- [8] Aizawa K, Tomimitsu H, Tamaki H and Yoshinari A 2000 *Journal of Applied Crystallography* **33** 847-850
- [9] Durand-Charre M 1997 *The Microstructure of Superalloys* (Amsterdam, The Netherlands: Gordon and Breach Science Publishers) p 5
- [10] Strunz P, Mortensen K and Janssen S 2004 *Physica B* **350** e783
- [11] Strunz P, Gilles R, Mukherji D and Wiedenmann A 2003 *J. Appl. Cryst.* **36** 854-859
- [12] Schelten J and Schmatz W 1980 *J. Appl. Cryst.* **13** 385-390